

Article

Resolving Entangled J_{H-H} -Coupling Patterns for Steroidal Structure Determinations by NMR Spectroscopy

Danni Wu ¹, Kathleen Joyce Carillo ^{1,2,3}, Jiun-Jie Shie ¹ , Steve S.-F. Yu ¹  and Der-Lii M. Tzou ^{1,4,*} 

¹ Institute of Chemistry, Academia Sinica, Nankang, Taipei 11529, Taiwan; tomo20170414@gmail.com (D.W.); kjarillo@yahoo.com (K.J.C.); shiej@gate.sinica.edu.tw (J.-J.S.); Sfyu@gate.sinica.edu.tw (S.S.-F.Y.)

² International Graduate Program, SCST, Academia Sinica, Nankang, Taipei 11529, Taiwan

³ The Department of Applied Chemistry, National Yang Ming Chiao Tung University, Hsinchu 30013, Taiwan

⁴ Department of Applied Chemistry, National Chia-Yi University, Chia-Yi 60004, Taiwan

* Correspondence: Tzougate@gate.sinica.edu.tw

Abstract: For decades, high-resolution ^1H NMR spectroscopy has been routinely utilized to analyze both naturally occurring steroid hormones and synthetic steroids, which play important roles in regulating physiological functions in humans. Because the ^1H signals are inevitably superimposed and entangled with various J_{H-H} splitting patterns, such that the individual ^1H chemical shift and associated J_{H-H} coupling identities are hardly resolved. Given this, applications of this information for elucidating steroidal molecular structures and steroid/ligand interactions at the atomic level were largely restricted. To overcome, we devoted to unraveling the entangled J_{H-H} splitting patterns of two similar steroidal compounds having fully unsaturated protons, i.e., androstanolone and epiandrosterone (denoted as **1** and **2**, respectively), in which only hydroxyl and ketone substituents attached to C3 and C17 were interchanged. Here we demonstrated that the J_{H-H} values deduced from **1** and **2** are universal and applicable to other steroids, such as testosterone, 3β , 21-dihydroxyprogesterone, prednisolone, and estradiol. On the other hand, the ^1H chemical shifts may deviate substantially from sample to sample. In this communication, we propose a simple but novel scheme for resolving the complicated J_{H-H} splitting patterns and ^1H chemical shifts, aiming for steroidal structure determinations.

Keywords: steroid hormones; proton chemical shifts; J scalar coupling constants; structural determinations; fingerprint patterns



Citation: Wu, D.; Carillo, K.J.; Shie, J.-J.; Yu, S.S.-F.; Tzou, D.-L.M. Resolving Entangled J_{H-H} -Coupling Patterns for Steroidal Structure Determinations by NMR Spectroscopy. *Molecules* **2021**, *26*, 2643. <https://doi.org/10.3390/molecules26092643>

Academic Editor:
Pierangela Ciuffreda

Received: 6 April 2021
Accepted: 29 April 2021
Published: 30 April 2021

Publisher's Note: MDPI stays neutral with regard to jurisdictional claims in published maps and institutional affiliations.



Copyright: © 2021 by the authors. Licensee MDPI, Basel, Switzerland. This article is an open access article distributed under the terms and conditions of the Creative Commons Attribution (CC BY) license (<https://creativecommons.org/licenses/by/4.0/>).

1. Introduction

It is well accepted that one-dimensional (1D) ^1H NMR spectroscopy serves as the most popular and quantitative analytical tool for small molecules [1] as well as for metabolomics [2–4]. The resulting ^1H NMR spectra reveal distinct ^1H spectral patterns for identifying the molecular structure and yet very often they are superimposed and coupled with neighboring spins via spin–spin scalar interactions. Typically, in steroidal compounds, resulting from the spin–spin couplings among adjacent ^1H nuclei, the ^1H signals are superimposed on each other and thereby convoluted severely with various scalar (J_{H-H} ; spin–spin) coupling patterns. As an outcome, it is extremely difficult to identify each of their ^1H resonances as well as the corresponding J_{H-H} coupling constants. Although the ^1H NMR spectroscopy acts as an important tool in analyzing molecular structure and dynamics at atomic resolution, and yet its applications to steroidal compounds are still limited.

Regardless of structural similarity, steroid hormones mediate a variety of physiological functions in humans [5–9]. In the steroid hormones, their ^1H spectra are actually quite different from one another. Each ^1H nucleus exists in a unique but slightly different local environment such that the associated scalar coupling pattern is made of either a doublet or a multiple of doublets. For those ^1H signals that are partially overlapped or superimposed,

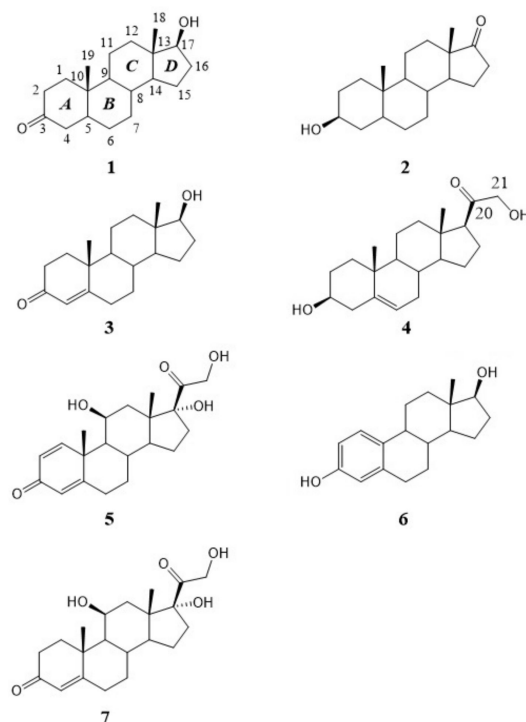
one has to make additional efforts and tedious measurements to resolve. Conventionally, one needs to apply traditional two-dimensional (2D) heteronuclear correlation spectroscopy, such as heteronuclear single-quantum correlation (HSQC) [10], heteronuclear multiple bond correlation (HMBC) [11], and homonuclear correlation spectroscopy (COSY) [12] experiments, to verify each of the ^1H chemical shifts and to unravel associated $J_{\text{H-H}}$ coupling constants. Aside from the traditional 2D NMR experiments, 2D $J_{\text{H-H}}$ -resolved spectroscopy is available for better resolving the $J_{\text{H-H}}$ splitting patterns in various schemes, for details see review article [13] and references therein. These $J_{\text{H-H}}$ -resolved 2D methods are aimed at detecting $J_{\text{H-H}}$ at the expense of signal sensitivity, which requires more measurement time than traditional 2D NMR experiments. Typically, a high field spectrometer (>600 MHz) is recommended to achieve higher spectral resolution. For interpretation of ^1H NMR spectra of complex compounds, in terms of their ^1H chemical shifts and $J_{\text{H-H}}$ coupling constants, an iterative ^1H Full Spin Analysis (HiFSA) method was first developed by Pauli and coworkers based on quantum mechanical calculations [14–16]. So far, there are no other alternatives that one can utilize to resolve ^1H chemical shifts and $J_{\text{H-H}}$ coupling constants, free from field strength-dependent measurements and/or laborious processes.

In this work, we initiate a new approach that allows one to uncover the superimposed ^1H chemical shifts as well as the $J_{\text{H-H}}$ coupling constants straightforwardly and reliably, aiming for structure determination.

2. Results

2.1. Chemical Shift Assignments

In the NMR spectra of steroidal compounds, the intrinsic $J_{\text{H-H}}$ coupling constants are basically invariant whereas their ^1H chemical shifts often vary substantially. For proof-of-concept, we selected two nearly identical steroidal compounds, i.e., compounds **1** and **2**, and measured their ^1H spectra for comparison. Molecular structures of **1** and **2** do show the same steroidal scaffold with slight modifications, in which the substituents attached to C3 and C17, i.e., ketone and hydroxyl groups, are interchanged (Scheme 1).



Scheme 1. Molecular structure of androstanolone (**1**), epiandrosterone (**2**), testosterone (**3**), 3β , 21-dihydroxyprogesterone (**4**), prednisolone (**5**), estradiol (**6**), hydrocortisone (**7**).

As demonstrated by the spectrum of **1** (Figure 1a), several ^1H signals are superimposed and entangled with multiple $J_{\text{H-H}}$ splitting patterns, in the ranges of $\delta = 0.9\text{--}1.0$, $1.05\text{--}1.09$, $1.33\text{--}1.5$, $1.55\text{--}1.65$, and $1.94\text{--}2.03$ ppm. Same for **2** (Figure 1c), more than half of the ^1H signals are seriously overlapped with multiple $J_{\text{H-H}}$ splitting patterns, in the ranges of $\delta = 1.0\text{--}1.1$, $1.15\text{--}1.47$, $1.53\text{--}1.72$, and $1.73\text{--}1.80$ ppm. Regardless of the structural similarity, the two spectra are so dissimilar and complicate that are difficult to assign.

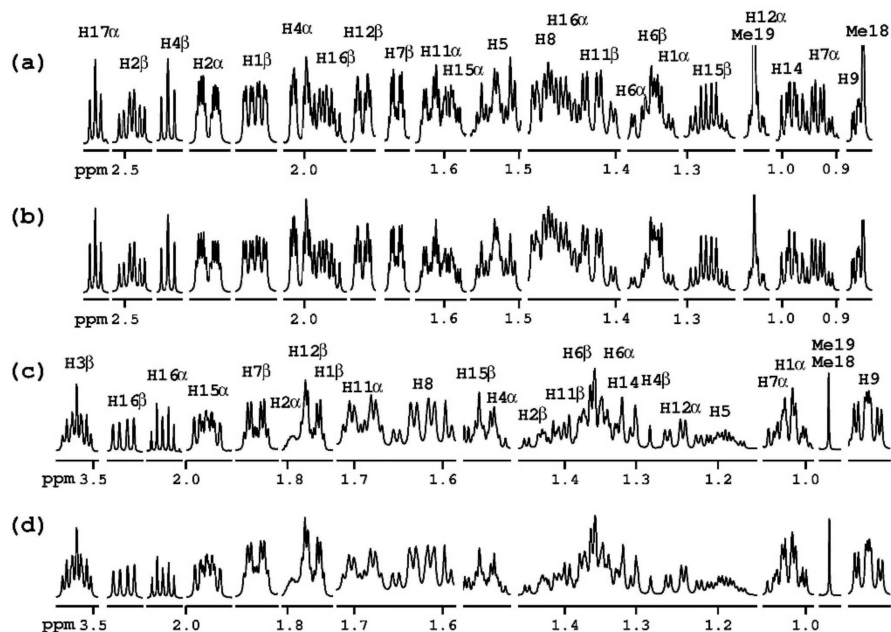


Figure 1. Solution NMR analysis of the steroidal compounds **1** and **2**. 1D ^1H spectrum of (a) **1** and (c) **2**. Note that **1** and **2** share a high degree of structural similarity (see Scheme 1), and yet their ^1H NMR spectra are rather dissimilar. In (a), half of the ^1H signals are superimposed and feature multiple $J_{\text{H-H}}$ splitting patterns, in the ranges of $\delta = 0.9\text{--}1.0$, $1.05\text{--}1.09$, $1.33\text{--}1.5$, $1.55\text{--}1.65$, and $1.94\text{--}2.03$ ppm. Whereas, in (c), more than half of the ^1H signals are overlapped and coupled with multiple $J_{\text{H-H}}$ splitting patterns, in the ranges of $\delta = 1.0\text{--}1.1$, $1.15\text{--}1.47$, and $1.53\text{--}1.80$ ppm. Given signal overlapping and the signal scrambling effect, the two spectral patterns are dissimilar. The ^1H chemical shift assignments were determined from the 2D HSQC experiment accordingly (Supporting Information Figures S1 and S2). (b,d) are a simulated spectrum of **1** and **2**, based on the ^1H chemical shift assignments and associated $J_{\text{H-H}}$ values (Table 1), using the Daisy software program (version 2.0.0 Bruker BioSpin GmbH, Rheinstetten, Germany); for details see text. For better clarity, these spectra are present on different scales.

Table 1. ^1H chemical shifts and $J_{\text{H-H}}$ coupling constants of **1** and **2**. ¹

Atom X	^1H Chemical Shift (ppm) ²			$J_{\text{X-Y}}$ (Hz)			Atom Y	
	(1)	(2)	Δ ³	(1)	(2)	Δ ⁴		
1 α (ax)	1.344	1.025	0.319	−13.1	−13.1	0.0	1 β	2J
				5.5	4.5	1.0	2 α	ax-eq
				14.2	14.2	0.0	2 β	ax-ax
1 β (eq)	2.061	1.754	0.307	2.6	2.6	0.0	2 α	eq-eq
				6.7	3.5	3.2	2 β	eq-ax
2 α (eq)	2.221	1.782	0.439	−15.2	−12.5	−2.7	2 β	2J
				NA	4.4		3	eq-eq
				2.6	2.1	0.5	4 α	4J
2 β (ax)	2.494	1.418	1.076	NA	11.6		3	ax-eq
3 (eq)	NA	3.530		NA	5.0		4 α	eq-eq
				NA	10.9		4 β	eq-ax

Table 1. Cont.

Atom X	¹ H Chemical Shift (ppm) ²			<i>J</i> _{X-Y} (Hz)			Atom Y	
	(1)	(2)	Δ ³	(1)	(2)	Δ ⁴		
4 α (eq)	2.006	1.556	<u>0.450</u>	−14.9	−12.5	<u>−2.4</u>	4 β	² <i>J</i>
				4.0	3.5	0.5	5	eq-ax
4 β (ax)	2.376	1.307	<u>1.069</u>	14.0	12.5	<u>1.5</u>	5	ax-ax
5 (ax)	1.526	1.173	<u>0.353</u>	4.0	4.0	0.0	6 α	ax-eq
				11.7	12.0	−0.3	6 β	ax-ax
6 α (eq)	1.350	1.358	−0.008	−12.0	−12.0	0.0	6 β	² <i>J</i>
				5.5	4.0	<u>1.5</u>	7 α	eq-ax
				3.0	3.0	0.0	7 β	eq-eq
6 β (ax)	1.358	1.359	−0.001	12.0	13.0	<u>−1.0</u>	7 α	ax-ax
				3.5	3.5	0.0	7 β	ax-eq
7 α (ax)	0.934	1.046	−0.112	−13.0	−13.0	0.0	7 β	² <i>J</i>
				12.0	12.0	0.0	8	ax-ax
7 β (eq)	1.730	1.847	−0.117	4.2	4.2	0.0	8	eq-ax
8 (ax)	1.486	1.628	−0.142	11.0	11.0	0.0	9	ax-ax
				10.8	10.8	0.0	14	ax-ax
9 (ax)	0.766	0.750	0.016	4.0	4.0	0.0	11 α	ax-eq
				12.6	12.6	0.0	11 β	ax-ax
11 α (eq)	1.625	1.691	−0.066	−13.7	−13.7	0.0	11 β	² <i>J</i>
				4.0	4.0	0.0	12 α	eq-ax
				3.0	3.0	0.0	12 β	eq-eq
11 β (ax)	1.426	1.384	0.042	13.4	13.4	0.0	12 α	ax-ax
				4.2	4.2	0.0	12 β	ax-eq
12 α (ax)	1.063	1.235	−0.172	−12.5	−12.5	0.0	12 β	² <i>J</i>
12 β (eq)	1.848	1.759	0.089					
14 (ax)	0.982	1.330	<u>−0.348</u>	7.7	5.8	<u>1.9</u>	15 α	³ <i>J</i>
				11.8	12.6	−0.8	15 β	³ <i>J</i>
15 α	1.593	1.961	<u>−0.368</u>	−12.8	−11.9	−0.9	15 β	² <i>J</i>
				3.7	8.6	<u>−4.9</u>	16 α	³ <i>J</i>
				9.8	1.0	<u>8.8</u>	16 β	³ <i>J</i>
15 β	1.268	1.566	<u>−0.298</u>	12.3	9.2	<u>3.1</u>	16 α	³ <i>J</i>
				6.0	9.0	<u>−3.0</u>	16 β	³ <i>J</i>
16 α	1.456	2.072	<u>−0.616</u>	−13.5	−19.2	<u>5.7</u>	16 β	² <i>J</i>
				8.4	NA		17 α	³ <i>J</i>
16 β	1.973	2.440	<u>−0.467</u>	9.0	NA		17 α	³ <i>J</i>
17 α	3.573	NA						
Me-18	0.773	0.887	−0.114					
Me-19	1.088	0.887	<u>0.201</u>					

¹H chemical shifts are in units of ppm, within an uncertainty of ± 0.001 ppm. The sample was dissolved in CD₃OD and examined by AV600. ² Solution ¹H NMR chemical shift assignments determined from HSQC, HMBC, and COSY experiments. ³ Chemical shift differences (Δ) between 1 and 2 greater than 0.2 ppm or equal are underlined. ⁴ *J*_{H-H} coupling constant differences (Δ) between 1 and 2 greater than 1.0 Hz or equal are underlined.

Figure 1. Solution NMR analysis of the steroidal compounds 1 and 2. 1D ¹H spectrum of (a) 1 and (c) 2. Note that 1 and 2 share a high degree of structural similarity (see Scheme 1), and yet their ¹H NMR spectra are rather dissimilar. In (a), half of the ¹H signals are superimposed and feature multiple *J*_{H-H} splitting patterns, in the ranges of $\delta = 0.9$ –1.0, 1.05–1.09, 1.33–1.5, 1.55–1.65, and 1.94–2.03 ppm. Whereas, in (c), more than half of the ¹H signals are overlapped and coupled with multiple *J*_{H-H} splitting patterns, in the ranges of $\delta = 1.0$ –1.1, 1.15–1.47, and 1.53–1.80 ppm. Given signal overlapping and the signal scrambling effect, the two spectral patterns are dissimilar. The ¹H chemical shift assignments were determined from the 2D HSQC experiment accordingly (Supporting Information Figure S1 and S2). (b,d) are a simulated spectrum of 1 and 2, based on the ¹H chemical shift assignments and associated *J*_{H-H} values (Table 1), using the Daisy software program (version 2.0.0 Bruker BioSpin GmbH, Rheinstetten, Germany); for details see text. For better clarity, these spectra are present on different scales.

To facilitate the chemical shift assignments, we then conducted 2D $^1\text{H}/^{13}\text{C}$ HSQC and DEPT experiments to identify the ^1H and ^{13}C chemical shifts of **1** and **2** (see Supplementary Figures S1–S4), respectively. The ^1H chemical shifts were further confirmed by 2D HMBC and COSY (correlation spectroscopy) experiments (Figures S5–S8). Both the ^1H and ^{13}C chemical shift assignments were determined (Table 1 and Table S1). To confirm the spectral dissimilarity is mainly due to ^1H chemical shift differences but not associated $J_{\text{H-H}}$ coupling constant variations, we also carried out an iterative simulation analysis to unravel the $J_{\text{H-H}}$ values of **1** and **2** (Table 1), respectively, to be elaborated below. As suggested, most of their ^1H chemical shifts (18 out of 24) differ by 0.1–1.0 ppm, equivalent to 50–500 Hz as measured by a 500 MHz spectrometer. In contrast, most of the $J_{\text{H-H}}$ values remained basically invariant. There are only a few residues in rings *A* and *D*, indicating deviations in the range of 0.3–5.7 Hz. Thus, it was confirmed that the spectral dissimilarity between **1** and **2** is primarily due to the ^1H chemical shift deviations, but not the variations of the $J_{\text{H-H}}$ coupling constants.

2.2. Resonance Hopping Effect

Note that the ^1H resonances of **1** and **2** display different sequential ordering from the downfield to upfield regions. In the case of **1**, as revealed by steroidal ring *B*, the signals arising from H7 β (1.730 ppm), H5 (1.526 ppm), H8 (1.486 ppm), H6 β (1.358 ppm), H6 α (1.350 ppm), H7 α (0.934 ppm) and H9 (0.766 ppm) displayed in descending order. Whereas in **2**, the same signals followed a dissimilar sequential ordering, i.e., H7 β (1.847 ppm), H8 (1.628 ppm), H6 β (1.359 ppm), H6 α (1.358 ppm), H5 (1.173 ppm), H7 α (1.046 ppm), and H9 (0.750 ppm). We termed this as a resonance hopping effect or sequential disordering effect. As suggested, a modification of certain substituents, in this case, an interexchange of ketone and hydroxyl groups, could lead to a substantial change of the chemical environment in remote and non-related sites. For example, the hopping effect was also detected from those signals arising from steroidal ring *C* as well, i.e., H12 β (1.848 ppm in **1** and 1.759 ppm in **2**), H15 α (1.593 ppm in **1** and 1.961 ppm in **2**), H12 α (1.063 ppm in **1** and 1.235 ppm in **2**), and H14 (0.982 ppm in **1** and 1.330 ppm in **2**). Notice that the ^1H chemical shifts of **1** and **2** vary in a wide range from -0.62 to $+0.107$ ppm, not limited to rings *A* and *D*. Given this hopping effect, aside from the signal superimpositions, the signal assignments of **1** and **2** are rather complicated.

2.3. Fingerprint Pattern Identification

In steroidal compounds, each ^1H nucleus is experienced in a unique chemical environment, in which the respective scalar coupling pattern is made of either a doublet or a multiple of doublets, depending on the adjacent ^1H nuclei. As reported in the literature [17,18], each ^1H signal typically is involved three to four spin-spin couplings of different “sizes”. And the overall splitting pattern is mainly dependent on the number of the $J_{\text{H-H}}$ coupling constants and their sizes. As referring to the size variations in a unit of Hz, the geminal coupling constants ($^2J_{\text{gem}}$) distributed in the range of -12 to -14 Hz, the axial-axial coupling constants ($^3J_{\text{ax-ax}}$) vary within 10.5 to 14.5 Hz, the axial-equatorial coupling constants ($^3J_{\text{ax-eq}}$) within 3.5 to 5.0 Hz, the equatorial-equatorial coupling constants ($^3J_{\text{eq-eq}}$) near 3.0 Hz, as well as other ($^4J_{\text{H-H}}$) coupling constants below 3–4 Hz. To facilitate $J_{\text{H-H}}$ coupling constant determinations, we here divided the $J_{\text{H-H}}$ values of steroids into four categories based on their “sizes”, namely large (14–10 Hz), medium-large (9–6 Hz), medium (5–3 Hz) and small (below 3 Hz). As revealed in Figure 2, various scenarios, including “doublet” of “quartets”, “triplet” of “doublets”, and “triplet” of “quartets”, are representative of the $J_{\text{H-H}}$ values of certain combinations. In the light of the distinct spectral patterns, one can identify the associated $J_{\text{H-H}}$ coupling constants directly from its 1D spectrum. For example, the H1 β signal of **1** (Figure 1a) resembles that of “doublet” of “quartets” pattern (Figure 2b), and the H12 α signal of **2** (Figure 1c) is quite similar to that of “triplet” of “doublets” feature (Figure 2e).

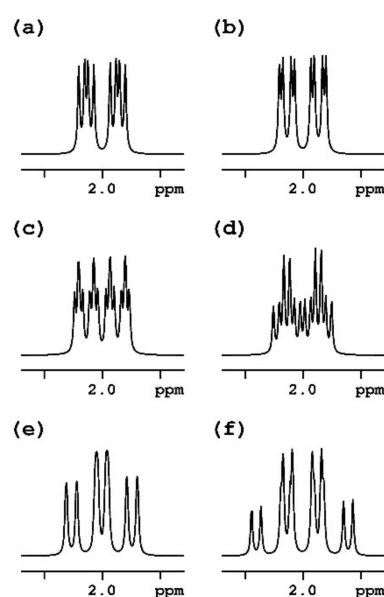


Figure 2. Characteristic multiple doublet fingerprint patterns observable from steroidal compounds. Simulations of splitting patterns in various J_{H-H} combinations: (a) 13.5, 4.0, 2.5 Hz; (b) 13.5, 5.0, 1.5 Hz; (c) 13.5, 6.5, 2.0, 1.5 Hz; (d) 13.5, 4.5, 4.5, 2.5 Hz; (e) 13.5, 12.5, 4.5, 0.5 Hz, and (f) 13.5, 13.5, 12.5, 4.0 Hz. Notice that the distinct splitting patterns are strictly dependent on the number and the “size” of J_{H-H} values. For brevity, the J_{H-H} values were divided into four categories that differed in size, i.e., large (14–10 Hz), medium-large (9–6 Hz), medium (5–3 Hz), and small (below 3 Hz). As revealed by the distinct splitting patterns, one can deduce the associated J_{H-H} values accordingly; for details see text.

For those ^1H signal patterns free from any signal overlap, one can follow the above-mentioned simulation analysis to deduce the J_{H-H} values directly. For those signals with partial or serious overlap, one needs to pay extra efforts to verify manually possible scenarios in different combinations of chemical shifts and J_{H-H} values, which is considered labor-intensive and time-consuming. For this, we proposed an iterative simulation scheme for unraveling the ^1H chemical shifts and the J_{H-H} values stepwise, to be elaborated below.

2.4. Resolving Entangled J_{H-H} Coupling Patterns

Because of the spectral complexity, it is highly advisable to resolve the J_{H-H} coupling constants stepwise, first starting from those signals free from signal overlap, then moving on to those with partial signal overlap, and finally to those with serious signal overlap. As suggested, one shall first eliminate impossible combinations and then worked on the simulation for better fitting of the experimental spectrum. Having the chemical shifts deduced from the 2D HSQC spectra, we then uncovered the entangled J_{H-H} splitting patterns iteratively. In the 1D spectra of **1** and **2** (Figure 1a,c), the most difficult part arose from those ^1H signals with serious overlap, i.e., H8/H16 α /H11 β in **1** as well as H11 β /H6 β /H6 α /H14/H4 β in **2**. In these cases, we mainly focused on the uncovered upfield portion for simulation to extract the J_{H-H} coupling constants. With our great efforts, we achieved to determine the J_{H-H} coupling constants of **1** and **2**, respectively. As indicated, the simulated ^1H spectra of **1** and **2** (Figure 1b,d) are in good agreement with the experimental results (Figure 1a,c), indicating that the J_{H-H} values deduced from **1** and **2** are validated.

To validate whether the J_{H-H} values deduced from **1** and **2** apply to other steroidal compounds, we chose four steroidal compounds, i.e., testosterone (**3**), 3 β , 21-dihydroxypregna-5-en-20-one (**4**), prednisolone (**5**), and estradiol (**6**) (Scheme 1) for NMR spectral analysis. According to the J_{H-H} values deduced from **1** and **2** (Table 1) and the ^1H chemical shifts determined from their 2D HSQC spectrum (Figures S9–S12), we simulated the ^1H spectra and divided it into four subspectra, corresponding to rings A (H1–H5), B (H6–

H9), C (H11-H12), and D (H14-H17), respectively, to reduce the spectral overlaps. As displayed (Figure 3 and Figures S13–S15), the ^1H signals were better resolved such that one could identify characteristic spectral patterns. For example, similar spectral patterns were found in 1 and 3 (Figures 1a and 3), i.e., H7 α , H11 α , H11 β , H12 β , H14, H15 β , H16 β , and H17 α ; in 2 and 6 (Figure 2c and Figure S15), i.e., H3 β , H7 β , H9, H11 α , and H12 α ; in 4 and 5 (Figures S13 and S14), i.e., H1, H2, H4, H6 β , and H7 α , and in 3 and 5 (Figure 3 and Figure S14), i.e., H6 α and H7 α . For more applications, we then deduced several $J_{\text{H-H}}$ values from different ring structures (Table 2), in association with human steroid hormones [19].

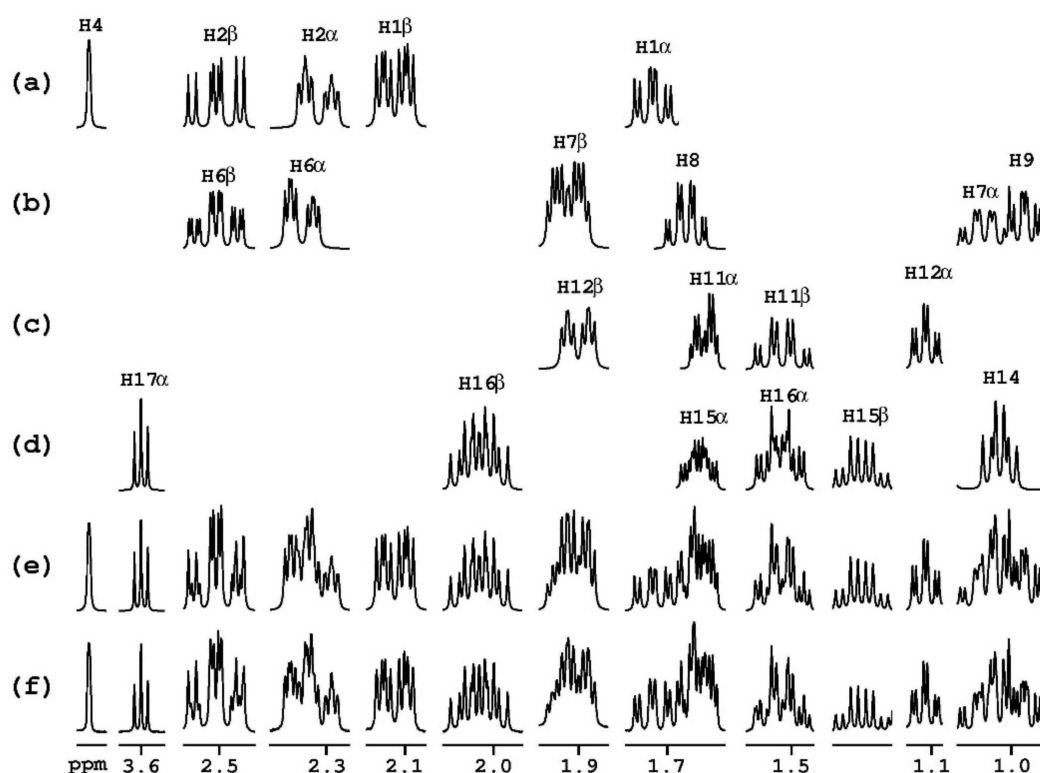


Figure 3. Characteristic ^1H NMR segmental spectra patterns of steroidal compounds. Four subspectra of 3 were generated using the Daisy software program, corresponding to steroidal rings (a) A, (b) B, (c) C, and (d) D, respectively. Given the ^1H chemical shifts deduced from the 2D HSQC measurements (Supporting Information Figure S9) and associated $J_{\text{H-H}}$ coupling constants determined from 1 and 2 (Table 1), the ^1H NMR subspectra were constructed, for details see text. Note that the spectral similarities can be identified in different steroidal compounds. (e) A summation of the four subspectra (a–d) in the simulation of the respective ^1H NMR spectrum. (f) Experimental ^1H NMR spectrum. For better clarity, the subspectra are presented on different scales.

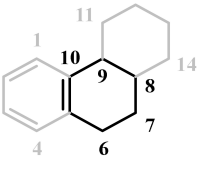
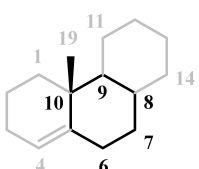
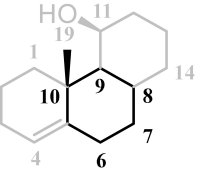
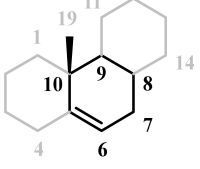
Table 2. $J_{\text{H-H}}$ coupling constants deduced from various steroidal ring combinations ¹.

Ring A							
X-Y	$J_{\text{X-Y}}$	X-Y	$J_{\text{X-Y}}$	X-Y	$J_{\text{X-Y}}$	X-Y	$J_{\text{X-Y}}$
1 α -1 β	-13.4	1 α -1 β	-13.5	1-2	10.1	1-2	8.4

Table 2. Cont.

1 α -2 α	3.9	1 α -2 α	4.8	1-19	0.5	2-4	2.5
1 α -2 β	14.1	1 α -2 β	15.0	2-4	2.0	4-6 β	0.6
1 α -19	0.8	1 α -19	0.5	4-6 β	1.3		
1 β -2 α	3.3	1 β -2 α	3.3				
1 β -2 β	3.8	1 β -2 β	5.2				
2 α -2 β	-12.7	2 α -2 β	-17.0				
2 α -3	4.3	2 α -4	1.0				
2 α -4 α	2.3	4-6 β	1.9				
2 β -3	11.4						
3-4 α	5.1						
3-4 β	11.5						
4 α -4 β	-13.0						
4 β -6	2.5						

Ring B

							
X-Y	J_{X-Y}	X-Y	J_{X-Y}	X-Y	J_{X-Y}	X-Y	J_{X-Y}
6 α -6 β	-17.5	6 α -6 β	-14.6	6 α -6 β	-13.6	6-7 α	2.1
6 α -7 α	5.5	6 α -7 α	4.2	6 α -7 α	4.7	6-7 β	5.5
6 α -7 β	2.0	6 α -7 β	2.4	6 α -7 β	1.9	6-4 β	2.5
6 β -7 α	12.0	6 β -7 α	14.1	6 β -7 α	13.5	7 α -7 β	-17.5
6 β -7 β	5.5	6 β -7 β	5.5	6 β -7 β	5.3	7 α -8	10.4
6 β -4	0.6	6 β -4	2.0	6 β -4	1.3	7 α -4 β	3.1
7 α -7 β	-12.8	7 α -7 β	-12.9	7 α -7 β	-13.5	7 β -8	5.1
7 α -8	12.0	7 α -8	11.9	7 α -8	12.3	7 β -4 β	2.7
7 β -8	3.0	7 β -8	3.3	7 β -8	4.5	8-9	11.1
8-9	10.7	8-9	10.7	8-9	11.1	8-14	10.6
8-14	12.3	8-14	10.9	8-14	10.9	9-11 α	4.6
9-11 α	4.0	9-11 α	4.3	9-11	3.6	9-11 β	12.3
9-11 β	12.3	9-11 β	12.3				

Ring C

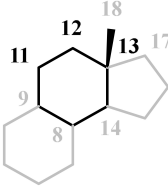
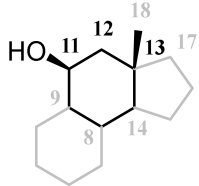
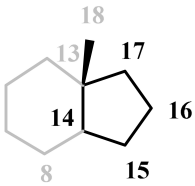
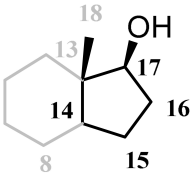
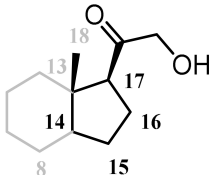
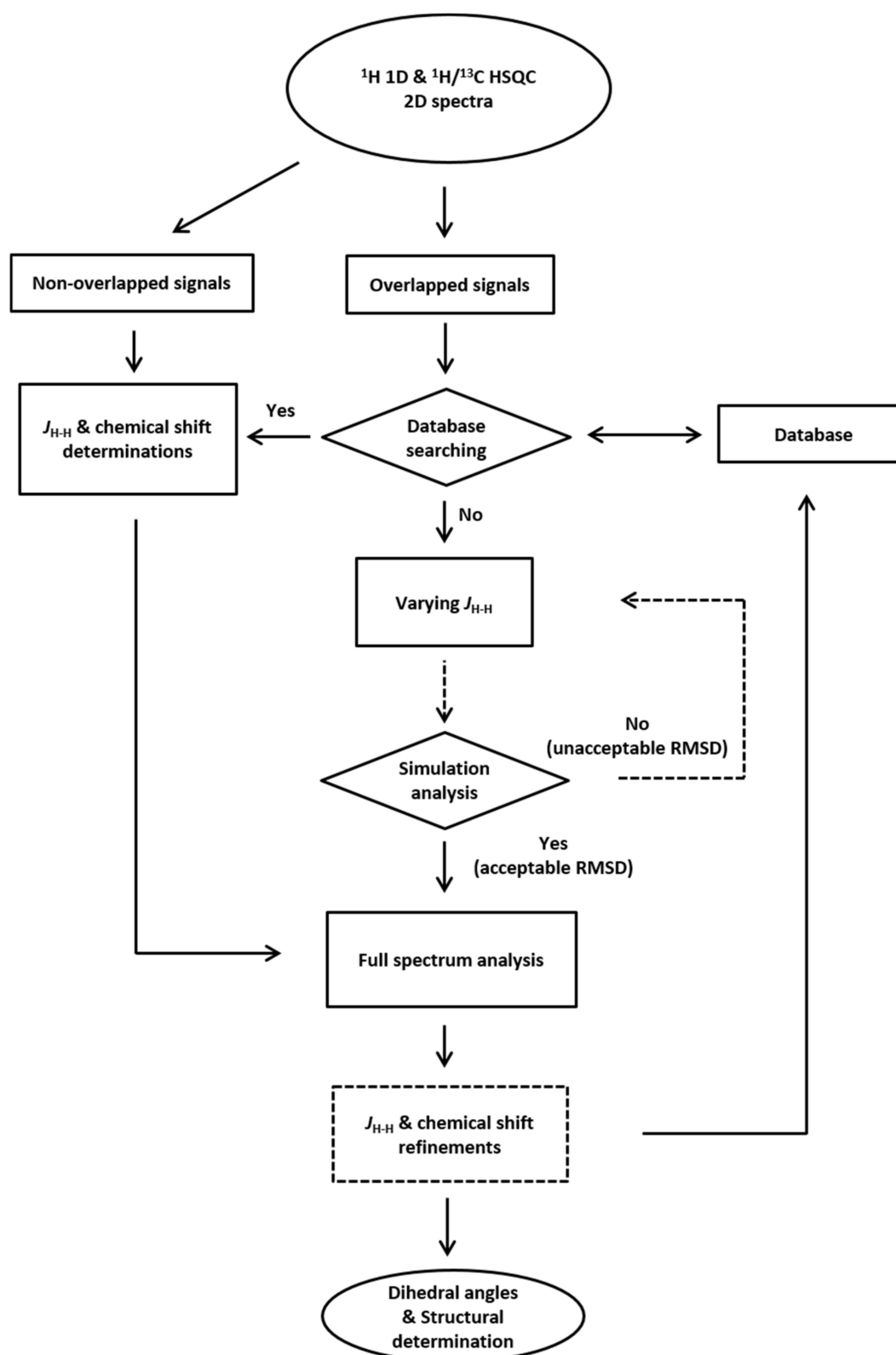
			
X-Y	J_{X-Y}	X-Y	J_{X-Y}
11 α -11 β	-13.3	11-9	4.0
11 α -9	4.3	11-12 α	3.7
11 α -12 α	4.3	11-12 β	2.6
11 α -12 β	2.7	12 α -12 β	-13.7
11 β -9	12.3	12 α -18	0.5
11 β -12 α	13.4	12 β -18	0.5
11 β -12 β	4.2		
12 α -12 β	-12.5		
12 α -18	0.5		

Table 2. Cont.

Ring D					
					
14-8	11.1	14-8	10.9	14-8	11.0
14-15 α	7.3	14-15 α	7.2	14-15 α	6.9
14-15 β	12.7	14-15 β	12.3	14-15 β	10.8
15 α -15 β	-11.6	15 α -15 β	-12.6	15 α -15 β	-12.5
15 α -16 α	10.1	15 α -16 α	3.5	15 α -16 α	9.8
15 α -16 β	3.0	15 α -16 β	9.5	15 α -16 β	3.0
15 β -16 α	6.8	15 β -16 α	11.9	15 β -16 α	6.1
15 β -16 β	12.1	15 β -16 β	5.9	15 β -16 β	12.0
16 α -16 β	-13.7	16 α -16 β	-13.7	16 α -16 β	-13.3
16 α -17 α	9.3	16 α -17	8.3	16 α -17	9.0
16 α -17 β	4.2	16 β -17	9.1	16 β -17	9.4
16 β -17 α	9.4				
16 β -17 β	2.9				
17 α -17 β	-12.5				

¹J_{X-Y} coupling constants were measured in units of Hz, within an uncertainty of ± 0.3 Hz.

Here we proposed a simple and iterative scheme for unraveling $J_{\text{H-H}}$ values, aiming for molecular structure determination by solution NMR spectroscopy (Scheme 2). In this scheme, we first measured 1D ¹H and 2D ¹H/¹³C HSQC spectra of the steroidal compound to be studied. For un-overlapped signals, both the chemical shifts and $J_{\text{H-H}}$ values can be determined straightforward, as described above. On the other hand, for each of the overlapped signals, one can identify how many ¹H signals are needed for database searching. Given their ¹H chemical shifts, we then carry out a simulation analysis for each of the overlapped spectral patterns in a stepwise manner, first starting from those with two signals, then moving on to those with three signals, and so on. If any spectral pattern fits well the experimental data, one can determine the chemical shifts and J values directly. If not, one has to follow the iterative loop process (labeled by dotted lines) to simulate each of the spectral patterns. Once it is done for all, we can put all the chemical shifts and $J_{\text{H-H}}$ values together to do a full spectrum analysis. In the final step, if necessary, one can manually adjust the ¹H chemical shifts and the $J_{\text{H-H}}$ values, including linewidths, to refine the simulated spectrum (Scheme 2). A high accuracy of ± 0.01 ppm for the ¹H chemical shift determination and ± 0.3 Hz for the $J_{\text{H-H}}$ value determinations are achievable (Figure S16). For time-saving, we here generated an abovementioned database to store the ¹H chemical shifts and the $J_{\text{H-H}}$ values of the known compounds, such as 1 and 2. Before start working on a “new” steroidal compound, one can first check the database whether any similar spectral pattern that are available and therefore can be used directly. Aside, it is possible to make use of structural similarity to predict ¹H chemical shifts of “new” compound out of the known compound. For example, presumably 3 and 5 are both known compounds available in the database and 7 is the new compound, one can make use of the ¹H chemical shifts from 3 (for ring A) and those from 5 (for rings B–D), as well as associated $J_{\text{H-H}}$ values (Table 2) to simulate the full spectrum for 7. As shown (Figure 4), by properly adjusting a few chemical shifts for better curve fitting, one can easily uncover their ¹H chemical shifts. It is highly expected that the database will grow rapidly, while more and more information to be included, which greatly facilitates the analysis.



Scheme 2. Flowchart of resolving J_{H-H} coupling constants as well as 1H chemical shifts of steroidal compounds aiming for structural determination. The spectral fitting analysis for each of the overlapped spectral patterns is labeled by dotted lines. If necessary, the J_{H-H} coupling constants, 1H chemical shifts, and linewidths are to be refined manually for better curve fitting.

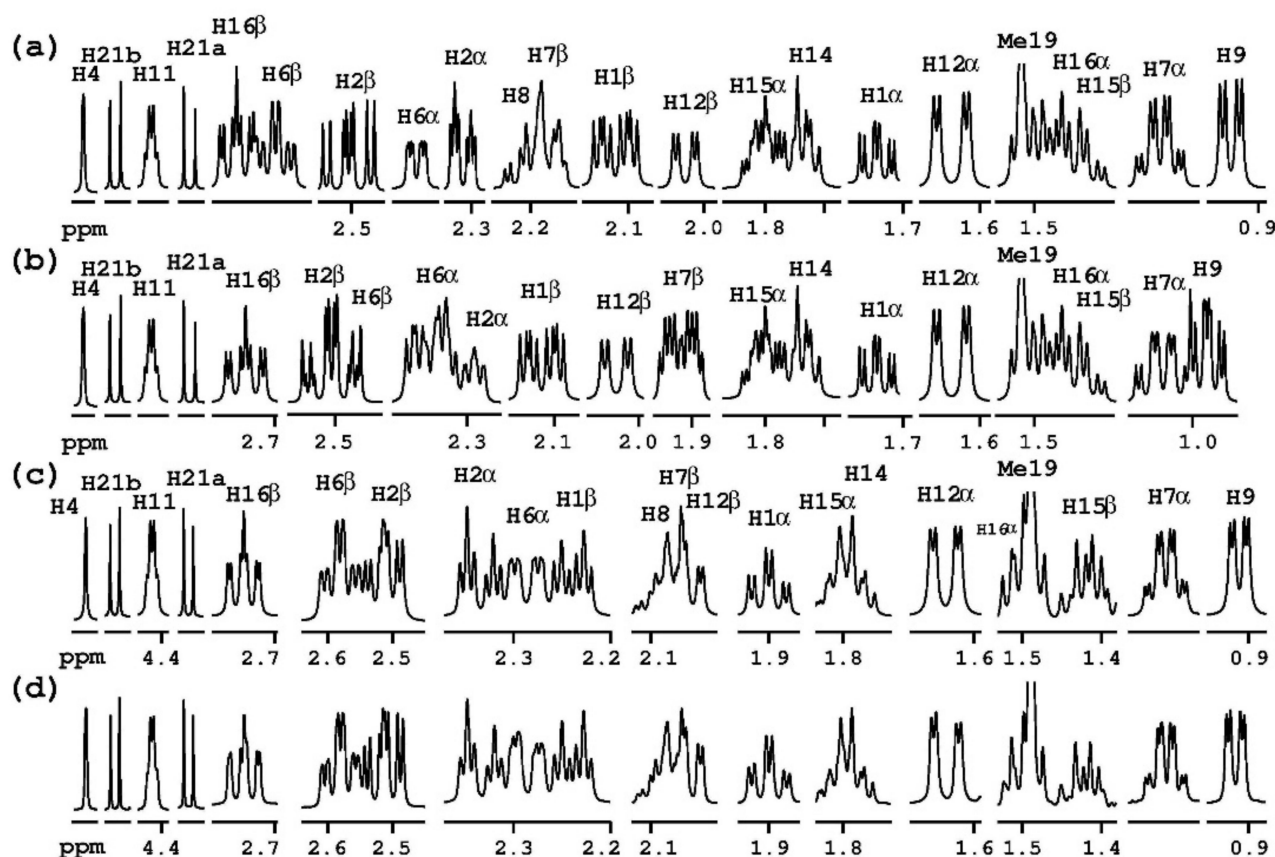


Figure 4. A ^1H NMR spectral simulation for hydrocortisone 7. The spectral simulation was made from the subspectra of 3 and 5 in different combinations. (a) A summation of the subspectra of 3 (ring A) and 5 (rings B–D). (b) A summation of the subspectra of 3 (rings A and B) and 5 (rings C and D). Comparing to that of (b), most of the signals of (a) are better correlated with that of the (d) experimental ^1H NMR spectrum with a few discrepancies, in which the H1 β , H1 α , and H16 α signals revealed downfield shifts whereas the H6 β , H6 α , H8, and H7 β signals exhibited upfield shifts. By appropriately adjusting these chemical shifts for better curve fitting, the resulting simulated spectrum (c) is nearly identical to the experimental (d).

2.5. Deducing Dihedral Angles and Structural Determinations

Using the Bothner-By equation [20], we calculated the dihedral angles of 1, 2, 3, 4, 5, and 7 from three-bond $J_{\text{H-H}}$ ($^3J_{\text{H-H}}$) values, respectively. These data are in good agreement with that extracted from their X-ray crystal structures (Tables S2–S7), with only a few exceptions seen in rings A and D showing deviations greater than 10° . The discrepancies were possibly due to electronegativity in the steroidal rings A and D. At the final step of the scheme, one can make use of the $^3J_{\text{H-H}}$ values to constitute the molecular structure of steroids or related compounds. In this work, we conducted an ab initio computer modeling simulation for 1, 2, 3, 4, 5, and 7 while setting their dihedral angles as angular constrains. Without violating the NOE distance constraints (Table S8), the most probable conformations resulting from the energy minimization in the simulation allow us to decipher its molecular structure accordingly. And the resulting molecular structures for compounds 1, 2, 3, 4, 5, and 7 (Figure 5) are in good agreements with that observed by X-ray crystallography [21–26]. Based on this, we claimed that the molecular structures resolved from the $^3J_{\text{H-H}}$ are validated.

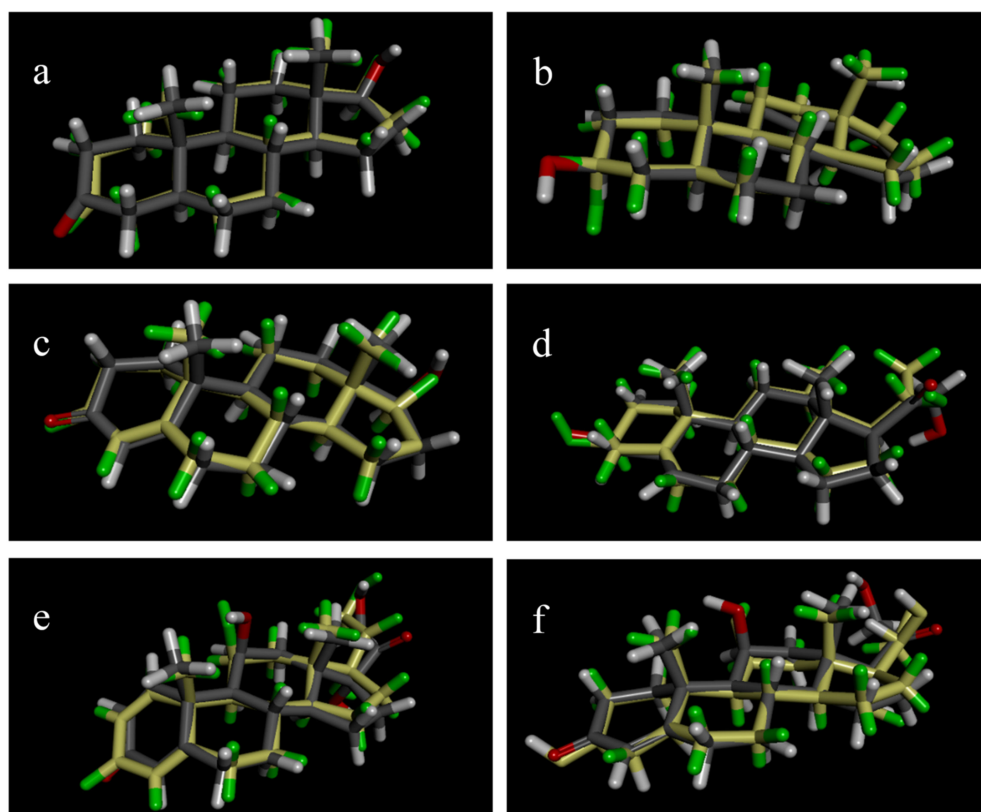


Figure 5. Molecular structure determination of steroidal compounds by computer simulation. The most probable conformations resulted from energy minimization calculation of six steroidal compounds, including (a) 1, (b) 2, (c) 3, (d) 4, (e) 5, and (f) 7, were presented. All the dihedral angles were deduced from three-bond $J_{\text{H-H}}$ values following the Bothner-By equation [20], for details see text. In the computer modeling simulation, no violation of the distance NOE constraints (Table S8) is allowed. For comparison, the X-ray structures of these compounds [21–25] are overlaid (colored in yellow and green). In the case of 4, because no X-ray structure is available, an X-ray structure of its analog 3β -hydroxygregn-5-en-20-one [26] was shown instead.

3. Discussion

Despite that steroidal compounds 1 and 2 are structurally similar, however, their ^1H NMR spectra are very different. To explain why, we devoted great efforts to analyze their ^1H chemical shifts and associated $J_{\text{H-H}}$ coupling constants, respectively. Here we reported that their $J_{\text{H-H}}$ coupling constants remain basically invariant, however, their ^1H chemical shifts deviate substantially. Due to the chemical shift deviations, it explains why their ^1H spectra are dissimilar. As believed, the $J_{\text{H-H}}$ coupling constants are universal and applicable to steroidal compounds as well as other organic compounds. Here we proposed a direct and simple approach for unraveling both $J_{\text{H-H}}$ coupling constants and ^1H chemical shifts of steroidal compounds. Making use of the $J_{\text{H-H}}$ values extracted from various steroidal structures, one can easily determine their ^1H chemical shifts without going through time-consuming 2D measurements and related data analysis.

It is anticipated that this NMR study approach will have a great impact in the field of steroidal conformational analyses and steroidal drug developments. In the application of steroid/metal ion chelation, we reported previously that ring D is responsible for the metal ion chelation and therefore its conformation is rather sensitive to the presence of metal ions, such as Mg^{2+} and Ca^{2+} [27]. By this means, one can probe steroidal conformational change due to the presence the metal ions. More conformational analyses of steroid/metal ion mixtures are currently undergoing in our lab. Apart from this, the simulation scheme we report here can be applicable for studying organic and inorganic compounds as well.

As demonstrated, the J_{H-H} coupling constants deduced from a certain type of organic or inorganic compounds remain in principle invariant, only the relevant ^1H chemical shifts might vary from sample to sample. By the same token, one can generate a set of ^1H chemical shift database of a related compound. It shall be aware that the spectral patterns measured at different magnetic field strengths are rather different because the chemical shifts are field strength dependent and yet the J_{H-H} coupling splitting are field strength independent. Aside, the ^1H signal patterns of organic or inorganic compounds are undoubtedly sensitive to salt concentration and solvent being used. To avoid spectral overlaps due to solvent signal, one can use deuterated methanol as D-solvent in the NMR measurements. Thus, it is advised to measure the spectra under the same condition throughout the study, including the magnetic field strength and the solvent as well.

4. Materials and Methods

4.1. Sample Preparation

The commercially available androstanolone, epiandrosterone, prednisolone, testosterone, estradiol and hydrocortisone (purity $\geq 99\%$) were purchased from Sigma-Aldrich (St. Louis, MO, USA) and used without further purification. Pregnenolone derivative, namely, 3β , 21-dihydroxypregna-5-en-20-one was synthesized based on the following procedure. Potassium carbonate (25 mg, 0.18 mmol) was added to a solution of 3β , 21-acetoxypregna-5-en-20-one (200 mg, 0.54 mmol) in anhydrous methanol (20 mL) and the resulting mixture stirred at room temperature for 1 h. The reaction mixture was quenched with acid resin and filtered. The residue was purified using column chromatography on silica gel (hexane/EtOAc:4/1) to afford the desired product (195 mg, 98%) as a white solid. mp 271–274 °C. (Lit. [28] 273–274.5 °C), TLC ($R_f = 0.37$, EtOAc/hexane = 1/1) ^1H NMR (500 MHz, CD_3OD): δ 5.37–5.33 (m, 1H, 6-H), 4.21 (d, $J = 19.4$ Hz, 1H, 21- H_b), 4.15 (d, $J = 19.4$ Hz, 1H, 21- H_a), 3.44–3.36 (m, 1H, 3-H), 2.59 (dd, $J = 10.2$ Hz, $J = 9.2$ Hz, 1H, 17-H), 2.28–2.23 (m, 1H, 4 α -H), 2.26–2.20 (m, 1H, 4 β -H), 2.22–2.14 (m, 1H, 16 β -H), 2.06–1.98 (m, 1H, 7 β -H), 1.97–1.91 (m, 1H, 12 β -H), 1.91–1.85 (m, 1H, 1 β -H), 1.84–1.77 (m, 1H, 2 α -H), 1.77–1.70 (m, 1H, 15 α -H), 1.75–1.66 (m, 1H, 16 α -H), 1.70–1.63 (m, 1H, 11 α -H), 1.63–1.55 (m, 1H, 7 α -H), 1.59–1.47 (m, 1H, 11 β -H), 1.58–1.52 (m, 1H, 2 β -H), 1.55–1.45 (m, 1H, 8-H), 1.47–1.39 (m, 1H, 12 α -H), 1.35–1.25 (m, 1H, 15 β -H), 1.25–1.17 (m, 1H, 14-H), 1.14–1.05 (m, 1H, 1 α -H), 1.03 (s, 3H, 19- CH_3), 1.05–0.97 (m, 1H, 9-H), 0.66 (s, 3H, 18- CH_3); ^{13}C NMR (125 MHz, CD_3OD): δ 212.1, 142.4, 122.4, 72.5, 70.3, 60.0, 58.3, 51.7, 45.7, 43.1, 39.9, 38.7, 37.9, 33.4, 33.1, 32.4, 25.8, 24.1, 22.3, 20.0, 13.9; HRMS (EI^+): m/z calcd for $\text{C}_{21}\text{H}_{32}\text{O}_3$: 332.2351; found: 332.2358.

4.2. NMR Experiments

Steroids were dried via lyophilization for 3 h to remove adsorbed moisture completely before NMR detection. Approximately 3 mg of sample was dissolved in 500 μL of anhydrous d_4 -methanol (Sigma-Aldrich, St. Louis, MO, USA) and analyzed using high-resolution NMR spectroscopy. For sake of consistency, all NMR measurements were performed on Bruker AV500 MHz spectrometer (Bruker BioSpin GmbH, Rheinstetten, Germany) equipped with a 5 mm z-gradient CryoProbe Prodigy BBO probe head at 298 K. All spectra were calibrated using the residual deuterated solvent signals as an internal reference (d_4 -methanol, ^1H δ 4.87 ppm; ^{13}C δ 49.15 ppm) and processed with Topspin 3.6 (Bruker BioSpin GmbH, Germany). For 2D experiments, $^1\text{H}/^1\text{H}$ homonuclear and $^1\text{H}/^{13}\text{C}$ heteronuclear chemical shift correlations were performed with the advanced version, including HSQC, HMBC, COSY, and nuclear Overhauser effect spectroscopy. The ^1H chemical shifts and J_{H-H} coupling constants were deduced from the ^1H NMR spectra via iterative full-spin analysis of steroids using the Daisy software package (Bruker BioSpin GmbH, Germany). The NMR subspectra were generated for steroidal rings of the steroidal compounds using the same software package.

4.3. Modelling of Steroid Structure and MD Simulation

Structures for compounds **1**, **2**, **3**, **4**, and **5** were retrieved from an online X-ray structure database while compound **7** structure was built using the GaussView software (version 4.1, Gaussian Inc., Wallingford, Connecticut, USA) [29,30]. Dihedral angles were initially set according to the calculated values from the J coupling constants. The OPLS-AA force field [29,30] was used for the simulation of all seven compounds. Using an OPLA force field basis model, simulation boxes containing the steroids and methanol solvents were generated. The GROMACS (2020.4) [31] package was employed as the MD engine to do the molecular dynamics simulations. All systems were analyzed comprising of the optimized steroid structures solvated with methanol inside a 5 nm cubic box. The system was initially subjected to energy minimization using the steepest descent method for 50,000 steps. The minimization step was followed by an equilibration step for 100 ps with a time-step of 2 femtoseconds at the canonical (NVT) ensemble while keeping the bonds for the steroids and methanol constrained using the LINCS algorithm. During NVT equilibration, the temperature of the system was maintained at 300 K. After NVT equilibration, it was followed by equilibration at an isothermal-isobaric (NPT) ensemble using the same parameters as in NVT equilibration while maintaining the system pressure at 1 bar using the Parrinello–Rahman isotropic coupling method. Afterward, MD simulations were then performed for all seven solvated steroid systems. After simulation, the final structure of the steroids was probed using GaussView 4.1, while setting the dihedral angles and the NOE data as angular and distance constraints, respectively.

Supplementary Materials: The following are available online, Figures S1 and S2: Solution $^1\text{H}/^{13}\text{C}$ 2D HSQC NMR spectrum of **1** and **2**, Figures S3 and S4: Solution $^1\text{H}/^{13}\text{C}$ DEPT NMR spectrum of **1** and **2**, Figures S5 and S6: Solution $^1\text{H}/^{13}\text{C}$ 2D HMBC NMR spectrum of **1** and **2**, Figures S7 and S8: Solution 2D COSY NMR spectrum of **1–2**, Figures S9–S12: Solution $^1\text{H}/^{13}\text{C}$ 2D HSQC NMR spectrum of **3–6**, Figures S13–S15: Characteristic ^1H NMR segmental spectra patterns of steroidal compound **4–6**, Figure S16: Superimpositions of multiple doublet splitting patterns of overlapped signals of prednisolone in various combinations, Table S1: ^{13}C chemical shift assignments of **1** and **2**, Tables S2–S7: Dihedral angles deduced from the vicinal $^3J_{\text{H-H}}$ coupling constants of **1–7**, Table S8: NOE constraints deduced from 2D NOESY experiments.

Author Contributions: Conceptualization: D.-L.M.T. and J.-J.S.; synthesis: D.W., investigation: D.W. and K.J.C.; methodology: D.W., K.J.C. and D.-L.M.T.; validation: S.S.-F.Y.; writing—original draft preparation: D.W. and K.J.C.; writing—review and editing: D.-L.M.T.; supervision: D.-L.M.T. and J.-J.S. All authors have read and agreed to the published version of the manuscript.

Funding: This research was funded by the Ministry of Science and Technology of Taiwan, grant MOST 108-2113-M-001-016 and 109-2113-M-001-030 (D.-L.M.T.).

Institutional Review Board Statement: Not applicable.

Informed Consent Statement: Not applicable.

Data Availability Statement: The data presented in this study are available on request from the corresponding author.

Acknowledgments: NMR spectra were collected at the Institute of Chemistry, Academia Sinica, and the High-field NMR Center (HFNMRC), Academia Sinica, supported by Academia Sinica Core Facility and Innovative Instrument Project (AS-CFII-108-112). We thank Claire Yang (Institute of Chemistry, Academia Sinica) for help in preparing the manuscript.

Conflicts of Interest: The authors declare there is no conflict of interest.

Sample Availability: Samples of the compounds are available from the authors.

References

1. Bharti, S.K.; Roy, R. Quantitative ^1H NMR spectroscopy. *TrAC Trends Anal. Chem.* **2012**, *35*, 5–26. [CrossRef]
2. Irwin, C.; Van Reenen, M.; Mason, S.; Mienie, L.J.; Wevers, R.A.; Westerhuis, J.A.; Reinecke, C.J. The ^1H -NMR-based metabolite profile of acute alcohol consumption: A metabolomics intervention study. *PLoS ONE* **2018**, *13*, e0196850. [CrossRef]

3. Gardner, A.; Parkes, H.G.; Carpenter, G.H.; So, P.-W. Developing and Standardizing a Protocol for Quantitative Proton Nuclear Magnetic Resonance (1H NMR) Spectroscopy of Saliva. *J. Proteome Res.* **2018**, *17*, 1521–1531. [CrossRef]
4. Lenz, E.M.; Wilson, I.D. Analytical Strategies in Metabonomics. *J. Proteome Res.* **2007**, *6*, 443–458. [CrossRef]
5. Kozlova, T.; Thummel, C.S. Steroid Regulation of Postembryonic Development and Reproduction in *Drosophila*. *Trends Endocrinol. Metab.* **2000**, *11*, 276–280. [CrossRef]
6. Morley, J.E. The politics of testosterone. *J. Sex. Med.* **2007**, *4*, 554–557. [CrossRef]
7. Maser, C.; Janssens, P.A.; Hanke, W. Stimulation of interrenal secretion in amphibia. I. Direct effects of electrolyte concentration on steroid release. *Gen. Comp. Endocrinol.* **1982**, *47*, 458–466. [CrossRef]
8. Enriori, P.J.; Enriori, C.L. The pathogenesis of osteoporosis in older women and men: A review. *J. Steroid Biochem. Mol. Biol.* **2002**, *82*, 1–6. [CrossRef]
9. Miner, J.N.; Chang, W.; Chapman, M.S.; Finn, P.D.; Hong, M.H.; Lopez, F.J.; Marschke, K.B.; Rosen, J.; Schrader, W.; Turner, R.; et al. An Orally Active Selective Androgen Receptor Modulator Is Efficacious on Bone, Muscle, and Sex Function with Reduced Impact on Prostate. *Endocrinology* **2007**, *148*, 363–373. [CrossRef]
10. Bodenhausen, G.; Ruben, D.J. Natural abundance nitrogen-15 NMR by enhanced heteronuclear spectroscopy. *Chem. Phys. Lett.* **1980**, *69*, 185–189. [CrossRef]
11. Bax, A.; Summers, M.F. Proton and carbon-13 assignments from sensitivity-enhanced detection of heteronuclear multiple-bond connectivity by 2D multiple quantum NMR. *J. Am. Chem. Soc.* **1986**, *108*, 2093–2094. [CrossRef]
12. Aue, W.P.; Bartholdi, E.; Ernst, R.R. Two-dimensional spectroscopy. Application to nuclear magnetic resonance. *J. Chem. Phys.* **1976**, *64*, 2229–2246. [CrossRef]
13. Lin, Y.; Zeng, Q.; Lin, L.; Chen, Z.; Barker, P.B. High-resolution methods for the measurement of scalar coupling constants. *Prog. Nucl. Magn. Reson. Spectrosc.* **2018**, *109*, 135–159. [CrossRef] [PubMed]
14. Napolitano, J.G.; Gödecke, T.; Rodríguez-Brasco, M.F.; Jaki, B.U.; Chen, S.-N.; Lankin, D.C.; Pauli, G.F. The Tandem of Full Spin Analysis and qHNMR for the Quality Control of Botanicals Exemplified with *Ginkgo biloba*. *J. Nat. Prod.* **2012**, *75*, 238–248. [CrossRef] [PubMed]
15. Napolitano, J.G.; Lankin, D.C.; McAlpine, J.B.; Niemitz, M.; Korhonen, S.-P.; Chen, S.-N.; Pauli, G.F. Proton Fingerprints Portray Molecular Structures: Enhanced Description of the 1H NMR Spectra of Small Molecules. *J. Org. Chem.* **2013**, *78*, 9963–9968. [CrossRef]
16. Pauli, G.F.; Chen, S.-N.; Lankin, D.C.; Bisson, J.; Case, R.J.; Chadwick, L.R.; Gödecke, T.; Inui, T.; Kronic, A.; Jaki, B.U.; et al. Essential Parameters for Structural Analysis and Dereplication by 1H NMR Spectroscopy. *J. Nat. Prod.* **2014**, *77*, 1473–1487. [CrossRef] [PubMed]
17. Becerra-Martínez, E.; Ramírez-Gualito, K.E.; Pérez-Hernández, N.; Joseph-Nathan, P. Total 1H NMR assignment of 3 β -acetoxypregna-5,16-dien-20-one. *Steroids* **2015**, *104*, 208–213. [CrossRef] [PubMed]
18. Hayamizu, K.; Kamo, O. Complete assignments of the 1H and 13C NMR spectra of testosterone and 17 α -methyltestosterone and the 1H parameters obtained from 600 MHz spectra. *Magn. Reson. Chem.* **1990**, *28*, 250–256. [CrossRef]
19. Hu, J.; Zhang, Z.; Shen, W.-J.; Azhar, S. Cellular cholesterol delivery, intracellular processing and utilization for biosynthesis of steroid hormones. *Nutr. Metab.* **2010**, *7*, 47. [CrossRef] [PubMed]
20. Bothner-By, A.A. Geminal and vicinal proton-proton coupling constants in organic compounds. In *Advances in Magnetic and Optical Resonance*; Waugh, J.S., Ed.; Academic Press: Cambridge, MA, USA, 1965; Volume 1, pp. 195–316.
21. Information, N.C.f.B. Androstanolone, Pubchem Compound Summary for Cid 10635. Available online: <https://pubchem.ncbi.nlm.nih.gov/compound/Androstanolone> (accessed on 4 February 2021).
22. Information, N.C.f.B. Epiandrosterone, Pubchem Compound Summary for Cid 441302. Available online: <https://pubchem.ncbi.nlm.nih.gov/compound/Epiandrosterone> (accessed on 4 February 2021).
23. Thakkar, A.L.; Jones, N.D.; Rose, H.A.; Tensmeyer, L.G.; Hall, N.A. Crystallographic data for testosterone hydrate and anhydrate. *Acta Crystallogr. Sect. B Struct. Crystallogr. Cryst. Chem.* **1970**, *26*, 1184. [CrossRef]
24. Suitchmezian, V.; Jess, I.; Sehnert, J.; Seyfarth, L.; Senker, J.; Näther, C. Structural, Thermodynamic, and Kinetic Aspects of the Polymorphism and Pseudopolymorphism of Prednisolone (11,17 α ,21-Trihydroxy-1,4-pregnadien-3,20-dion). *Cryst. Growth Des.* **2008**, *8*, 98–107. [CrossRef]
25. Roberts, P.J.; Coppola, J.C.; Isaacs, N.W.; Kennard, O. Crystal and molecular structure of cortisol (11 β ,17 α ,21-trihydroxypregn-4-ene-3,20-dione) methanol solvate. *J. Chem. Soc. Perkin Trans.* **1973**, *2*, 774–781. [CrossRef]
26. Bordner, J.; Hennessee, G.L.A.; Chandross, R.J. Pregnanes pr116 3b-hydroxy-s-pregnene-zo-one pregnenolone. *Cryst. Struct. Comm.* **1978**, *7*, 513–515.
27. Carillo, K.D.; Wu, D.; Lin, S.-C.; Tsai, S.-L.; Shie, J.-J.; Tzou, D.-L.M. Magnesium and calcium reveal different chelating effects in a steroid compound: A model study of prednisolone using NMR spectroscopy. *Steroids* **2019**, *150*, 108429. [CrossRef] [PubMed]
28. Hamilton, N.M.; Dawson, M.; Fairweather, E.E.; Hamilton, N.S.; Hitchin, J.R.; James, D.I.; Jones, S.D.; Jordan, A.M.; Lyons, A.J.; Small, H.F.; et al. Novel Steroid Inhibitors of Glucose 6-Phosphate Dehydrogenase. *J. Med. Chem.* **2012**, *55*, 4431–4445. [CrossRef] [PubMed]
29. Robertson, M.J.; Tirado-Rives, J.; Jorgensen, W.L. Improved Peptide and Protein Torsional Energetics with the OPLS-AA Force Field. *J. Chem. Theory Comput.* **2015**, *11*, 3499–3509. [CrossRef]

-
30. Jorgensen, W.L.; Maxwell, D.S.; Tirado-Rives, J. Development and Testing of the OPLS All-Atom Force Field on Conformational Energetics and Properties of Organic Liquids. *J. Am. Chem. Soc.* **1996**, *118*, 11225–11236. [[CrossRef](#)]
 31. Abraham, M.J.; Murtola, T.; Schulz, R.; Páll, S.; Smith, J.C.; Hess, B.; Lindahl, E. GROMACS: High performance molecular simulations through multi-level parallelism from laptops to supercomputers. *SoftwareX* **2015**, *1–2*, 19–25. [[CrossRef](#)]